Development 139, 2436-2446 (2012) doi:10.1242/dev.081547

Stable establishment of cotyledon identity during embryogenesis in *Arabidopsis* by *ANGUSTIFOLIA3* and *HANABA TARANU*

Mari Kanei[1], Gorou Horiguchi[2,3,*] and Hirokazu Tsukaya[1]

SUMMARY

In seed plants, the shoot apical and root apical meristems form at the apical and basal poles of the embryonic axis, and leaves form at the flanks of the shoot apical meristem. *ANGUSTIFOLIA3*/*GRF INTERACTING FACTOR1* (*AN3*/*GIF1*) encodes a putative transcriptional co-activator involved in various aspects of shoot development, including the maintenance of shoot apical meristems, cell proliferation and expansion in leaf primordia, and adaxial/abaxial patterning of leaves. Here, we report a novel function of AN3 involved in developmental fate establishment. We characterised an *an3*-like mutant that was found to be an allele of *hanaba taranu* (*han*), named *han-30*, and examined its genetic interactions with *an3*. *an3 han* double mutants exhibited severe defects in cotyledon development such that ectopic roots were formed at the apical region of the embryo, as confirmed by *pWOX5::GFP* expression. Additionally, *gif2* enhanced the ectopic root phenotype of *an3 han*. Although the auxin accumulation pattern of the embryo was correct in *an3 han-30*, based on *DR5rev::GFP* expression at the globular stage, expression of the *PLETHORA1* (*PLT1*), a master regulator of root development, expanded from the basal embryonic region to the apical region during the same developmental stage. Furthermore, the *plt1* mutation suppressed ectopic root formation in *an3 han*. These data suggest that establishing cotyledon identity requires both *AN3* and *HAN* to repress ectopic root formation by repressing *PLT1* expression.

KEY WORDS: Leaf development, Embryogenesis, Apical-basal patterning, *ANGUSTIFOLIA3*, *HANABA TARANU*, *Arabidopsis thaliana*

INTRODUCTION

All organs produced during plant development are classified into root, stem and aerial lateral organs (including leaf and floral organs). The sources of these organs are the shoot apical meristem (SAM) and root apical meristem (RAM), which are established during embryogenesis. In the post-globular stage of eudicot embryo development, cotyledons are formed at the apical end of the embryo, while SAM develops between the two cotyledons and RAM develops at the basal end of the embryo.

Organ identity is established by selecting a specific genetic program and repressing undesirable programs, typically through the action of transcription factors. Shoot and root identities are dependent on the establishment of SAM and RAM, and these meristems can be induced by overexpressing even a single transcription factor gene in *Arabidopsis thaliana* (hereafter, *Arabidopsis*). For example, ectopic SAM is induced in RAM by overexpressing *WUSCHEL* (*WUS*), a transcription factor gene that is essential for stem cell maintenance in shoots (Gallois et al., 2004). Likewise, the class III homeodomain leucine zipper (HD-ZIP III) transcription factors and AP2-domain transcription factors PLETHORA1 (PLT1) and PLT2 function as master regulators of embryonic apical fate and basal fate, respectively. When a microRNA-resistant *HD-ZIP III* gene is expressed in RAM, a second shoot pole is established instead of the embryonic root pole (Smith and Long, 2010). However, induction of *PLT* genes leads to ectopic root formation in the shoot apex (Aida et al., 2004; Galinha et al., 2007).

Preventing inappropriate fates is crucial during the developmental process. For normal embryonic root development, *HD-ZIP III* genes must be repressed (Grigg et al., 2009). Similarly, repression of *PLT* at the apical region by *TOPLESS* (*TPL*) is necessary for normal shoot development (Long et al., 2002; Long et al., 2006; Smith and Long, 2010). Establishment of the shoot-root axis is achieved by an antagonistic relationship between *HD-ZIP III* and *PLT* (Smith and Long, 2010). Repression of SAM-specific gene expression is important for normal leaf development. AS1 and AS2 suppress class I *KNOTTED-LIKE HOMEOBOX* (*KNOX*) genes during leaf development. This process induces determinate growth on the leaf primordium and differentiates the leaf primordium from SAM (Byrne et al., 2000; Ori et al., 2000; Semiarti et al., 2001; Lin et al., 2003; Guo et al., 2008). Recent studies have proposed a mechanism for preventing the SAM gene expression program from being activated in the leaf primordia by *YABBY* genes (Kumaran et al., 2002; Sarojam et al., 2010).

Despite this progress, the mechanisms that establish fundamental leaf identities are poorly understood. There are only two studies that show homeotic transformation of cotyledons into roots: one by the expression of either a dominant-negative version of Rab5 GTPase Ara7 or RNA interference of a Rab5-GEF gene, *AtVps9a* (Dhonukshe et al., 2008); and one by expressing constitutively active *RopGEF7* (Chen et al., 2011). In the former case, auxin response maxima at the tips of developing cotyledons were larger in transgenic plants than those in wild type (Dhonukshe et al., 2008).

[1]Department of Biological Sciences, Graduate School of Science, The University of Tokyo, 7-3-1 Hongo, Bunkyo-ku, Tokyo 113-0033, Japan. [2]Department of Life Science, College of Science, Rikkyo University, 3-34-1 Nishi-Ikebukuro, Toshima-ku, Tokyo 171-8501, Japan. [3]Research Center for Life Science, Rikkyo University, 3-34-1 Nishi-Ikebukuro, Toshima-ku, Tokyo 171-8501, Japan.

*Author for correspondence (ghori@rikkyo.ac.jp)

Accepted 29 April 2012

We have previously identified several factors contributing to leaf development. *ANGUSTIFOLIA3* (*AN3*)/*GRF-INTERACTING FACTOR1* (*GIF1*) encodes a putative transcriptional co-activator (Kim and Kende, 2004; Horiguchi et al., 2005). *an3* mutations lead to narrow leaves, owing to a significant reduction in cell number (Relichova, 1976; Kim and Kende, 2004; Horiguchi et al., 2005). AN3/GIF1 interacts with several members of GROWTH REGULATING FACTOR (GRF) and promotes cell proliferation in leaf primordia (Kim and Kende, 2004; Horiguchi et al., 2005). GIF and GRF families consist of three and nine members, respectively (Kim et al., 2003; Kim and Kende, 2004; Liu et al., 2009; Rodriguez et al., 2010). *GRF* and *GIF* members have redundant functions in determining lateral organ size (Kim et al., 2003; Kim and Kende, 2004; Lee et al., 2009). In the *GIF* family, *AN3*/*GIF1* plays a predominant role (Kim and Kende, 2004; Lee et al., 2009). Triple *gif* mutants have a more severe cell-proliferation defect in leaves and reduced floral organ number (Lee et al., 2009). Moreover, the *an3* mutation in combination with *miR396*-mediated silencing of most *GRF* family members causes the loss of SAM formation (Rodriguez et al., 2010).

Further characterisation of *an3* mutants revealed additional phenotypes. Compensation is an event that increases cell size in response to a reduction in leaf cell number due to a genetic defect (Tsukaya, 2002; Beemster et al., 2003; Tsukaya, 2008; Horiguchi and Tsukaya, 2011). The *an3*-induced compensation is mediated non-cell autonomously (Horiguchi et al., 2005; Ferjani et al., 2007; Fujikura et al., 2007; Fujikura et al., 2009; Lee et al., 2009; Kawade et al., 2010). AN3 is also involved in leaf patterning. The *an3* mutation enhances leaf polarity defects in *as1* and *as2* mutants (Horiguchi et al., 2011; Wang et al., 2011). This suggests that *AN3* plays a broad role in leaf developmental processes.

In this study, we further explored the developmental roles of *AN3*. To this end, we isolated a mutant (*#2047*) based on the phenotypic similarities to *an3*. The mutated gene in *#2047* was *HANABA TARANU* (*HAN*) (Zhao et al., 2004; Nawy et al., 2010). Our expression and genetic analyses demonstrated that the *an3 han* double mutants cause transformation of cotyledons into roots due to ectopic expression of *PLT1*. This suggests that the cooperative function of *AN3* and *HAN* is necessary to stably establish leaf identity in cotyledons and to repress root fate during embryogenesis.

MATERIALS AND METHODS

Plant materials and growth conditions

The wild-type accession used in this study was Col-0. The isolation of *#2047* mutant has been reported previously (Horiguchi et al., 2006). *han-1*, originally isolated in the Wassilewskija (Ws) background (Zhao et al., 2004), was back-crossed to Col-0 three times. The *gif2* mutant (SAIL_328_A03) has been reported previously (Lee et al., 2009). The T-DNA insertion mutants for *PLT1* and *GATA19* are SALK_116254 and SALK_138626, respectively (Alonso et al., 2003). The transgenic lines *DR5rev::GFP* (Friml et al., 2003) and *pWOX5::GFP* (Blilou et al., 2005) were crossed with *an3* and *#2047*. Seeds were sown on Murashige and Skoog (MS) inorganic salts (Murashige and Skoog, 1962) supplemented with Gamborg's B5 vitamins (Gamborg et al., 1968) and 2% (w/v) sucrose, and then solidified using 0.5% (w/v) gellan gum. Ten days after sowing, seedlings were transferred to rock wool (Nittobo, Tokyo, Japan) and watered daily with 0.5 g/l Hyponex solution (Hyponex Japan, Osaka, Japan). For the quantitative analysis of leaves, seeds were sown on rock wool. Plants were grown at 22°C under white fluorescent lamps (~50 μmol m^{-2} sec^{-1}) with a 16-hour light/8-hour dark cycle.

Microscopic observations

To measure the number and size of palisade mesophyll cells, we used the first leaves of plants 21 days after sowing (*n*=8). Leaves were fixed with FAA and cleared using chloral hydrate solution, as described previously (Tsuge et al., 1996). To observe petal epidermis cells, we examined the first three fully opened flowers on the primary meristem (*n*=10) by the dried-gel method, as described previously (Horiguchi et al., 2006). To determine cell size, whole leaf size and petal width, we used IMAGE J software (http://rsb.info.nih.gov/ij/). The average leaf area and cell size were estimated as previously described (Horiguchi et al., 2005). Seeds were removed from fruits and cleared with chloral hydrate solution (chloral hydrate: water: glycerol=8:2:1) on a microscope slide. Whole leaves, flowers, seeds and seedlings were observed using a stereoscopic microscope (MZ16F; Leica Microsystems, Tokyo, Japan). Leaf palisade cells, root cells, gel casts of petal epidermal cells and cleared embryos were observed under a Nomarski differential interference contrast microscope (DM4500B; Leica Microsystems). To observe reporter gene activity in embryos, the embryos were separated from seed coats and observed using a laser scanning confocal microscope (Meta510; Carl Zeiss, Tokyo, Japan). Representative images of homozygous *an3-4 han-30* embryos were chosen from self-pollinated *AN3/an3-4 han-30/han-30* or *an3-4/an3-4 HAN/han-30* plants.

Map-based cloning

The chromosomal position of the *#2047* mutation was mapped using F2 progenies derived from a cross between *an3 #2047* mutants and the Landsberg *erecta* accession. Genomic DNA was extracted from F2 progenies that exhibited abnormal seed shapes. Polymorphic DNA makers were designed according to data available from TAIR (http://www.arabidopsis.org).

In situ hybridisation

The *PLT1* and *PHABULOSA* (*PHB*) riboprobes were generated as described previously (Aida et al., 2004; Smith and Long, 2010). Digoxigenin-labelled sense and antisense RNA probes were synthesised with the DIG RNA labelling Kit (Roche Diagnostics, Tokyo, Japan) using T3 or T7 RNA polymerase (Roche Diagnostics). Embryos were fixed in 4% paraformaldehyde and 4% dimethyl sulfoxide in phosphate-buffered saline (PBS). Samples was dehydrated in an ethanol series, replaced with xylene, and embedded in Paraplast Plus (Sigma-Aldrich, Tokyo, Japan). Sections (8 μm) were placed on glass slides. The sections were fixed to glass slides by overnight incubation at 45°C. Pre-treatment was performed as described previously (Kouchi and Hata, 1993), except that protease K (1 μg/ml; Sigma-Aldrich) treatment was performed for 30 minutes at 37°C. Hybridisation was performed according to Nakayama et al. (Nakayama et al., 2010). For immunological detection, detection buffer containing NBT/BCIP (Roche Diagnostics) was added to each slide, incubated at 4°C overnight, and subsequently incubated at room temperature for at least 3 hours.

RESULTS

Isolation of mutants displaying an *an3*-like leaf phenotype

To search for novel factors related to *AN3* function, we first isolated mutants with an *an3*-like leaf shape (Horiguchi et al., 2006). The first leaves of wild-type plants developed nearly round leaf blades, whereas those of *an3* developed spoon-like leaves (Fig. 1A,B,E,F). Based on these phenotypic differences, we isolated only one recessive mutant with *an3*-like leaves, *#2047* (Fig. 1C,G). The leaf index (the ratio of leaf blade length to width) of the first leaves in *#2047* was 1.38 (*n*=8, s.d.=0.075), which was greater than the wild-type value of 1.28 (*n*=8, s.d.=0.065). The leaf index of *an3-4* was 1.73 (*n*=8, s.d.=0.060).

To examine leaf phenotype similarities between *#2047* and *an3* at a cellular level, we measured the number of palisade cells in the subepidermal layer (per leaf) and the size of palisade cells

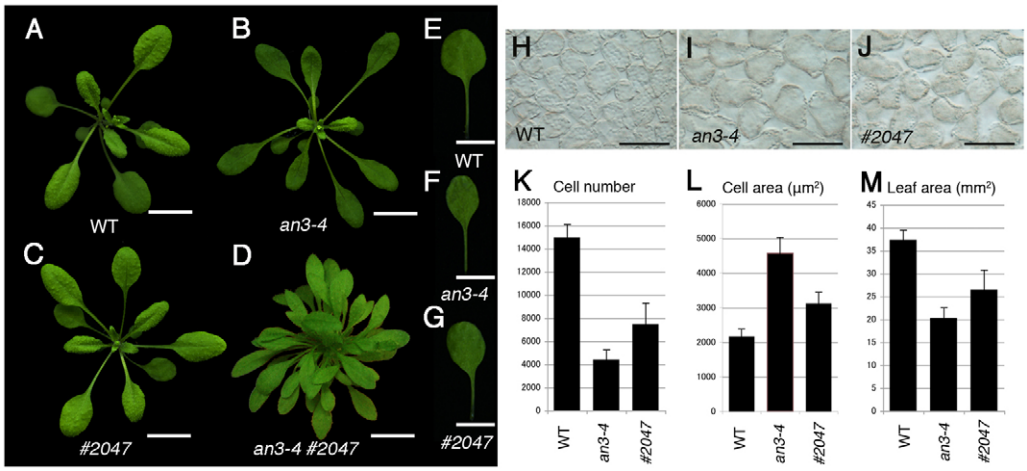

Fig. 1. Comparison of leaf phenotypes between *#2047* and *an3-4* mutants, and wild type. (**A-D**) Shoots of wild type (A), *an3-4* (B), *#2047* (C) and *an3-4 #2047* (D) grown for 21 days after sowing (DAS) (A-C) and 31 DAS (D). (**E-G**) First leaves of wild type (E), *an3-4* (F) and *#2047* (G) photographed at 21 DAS. (**H-J**) Paradermal view of palisade cells in the subepidermal layer in wild type (H), *an3-4* (I) and *#2047* (J). (**K-M**) The number of palisade cells in the subepidermal layer (K), the cell area of palisade cells (L) and leaf area (M). The first leaves from 21 DAS plants were analysed. Data are expressed as the mean±s.d. Scale bars: 1 cm in A-D; 5 mm in E-G; 100 μm in H-J.

using first leaves in *an3-4* (a null allele of *an3*) (Horiguchi et al., 2005) and *#2047* mutants. In *an3*, the reduced cell number induces enhanced cell expansion through non-cell-autonomous signalling (Horiguchi et al., 2005; Kawade et al., 2010). The cell numbers in *an3-4* and *#2047* were reduced to 29.5% and 49.9%, respectively, compared with wild type (Fig. 1K). In addition, palisade cell size increased in both mutants, by 75.7% and 32.9%, respectively, compared with wild type (Fig. 1H-J,L), demonstrating compensation in *#2047*. As a result, leaf blade area was reduced to only 54.3% and 70.9% in *an3-4* and *#2047*, respectively, compared with wild type (Fig. 1M). These results suggest that *#2047* has similar phenotypes to *an3-4* mutants at the cellular and organ level.

Additionally, variation in cotyledon number was observed in *#2047* seedlings with the three-cotyledon phenotype being most frequent (11.5%) (Fig. 2D,E; Table 1), which was rarely observed in *an3* alleles and wild type (Fig. 2A-C). *#2047* seedlings with fused cotyledons were also observed (data not shown).

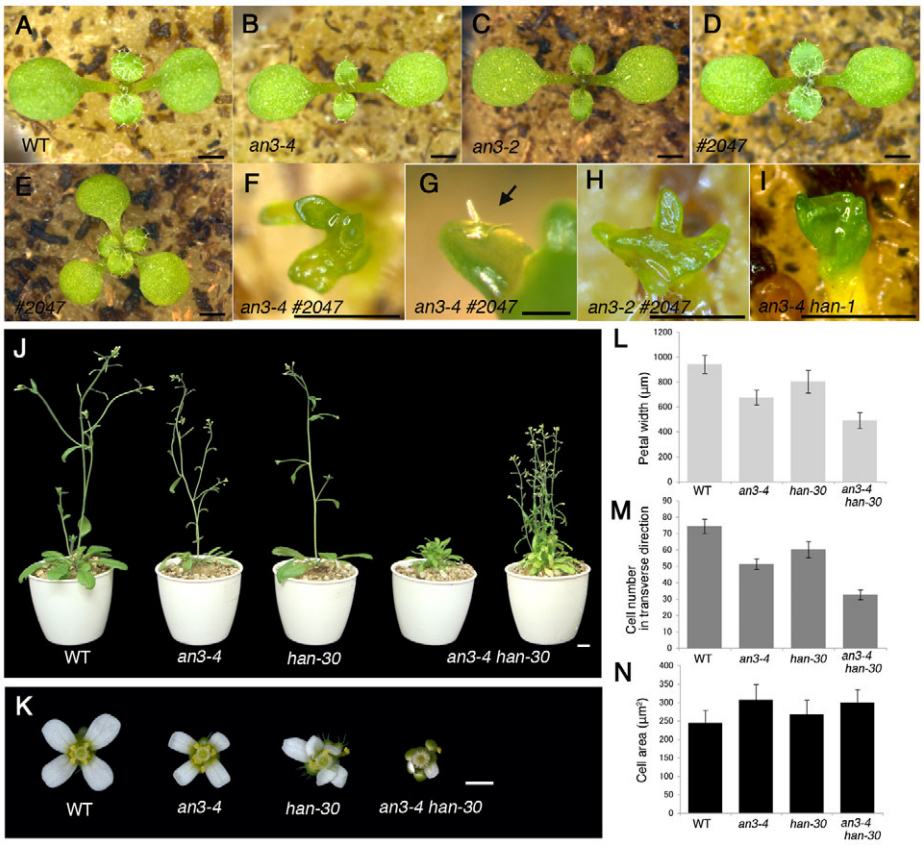

Fig. 2. Genetic interactions between *an3* and *#2047*. (**A-I**) The 9 DAS seedlings of wild type (A), *an3-4* (B), *an3-2* (C), *#2047* (D), *#2047* with a tricot phenotype (E) and *an3-4 #2047* (F,G), as well as 12 DAS *an3-2 #2047* seedlings (H) and 5 DAS *an3-4 han-1* seedlings (I). The arrow in G indicates a trichome produced on the protrusion of *an3-4 #2047*. (**J**) Gross morphology of wild type, *an3-4*, *han-30* and *an3-4 han-30* during the reproductive stage. All plants shown (except for the rightmost plant) are at 32 DAS. The rightmost one is *an3-4 han-30* at 44 DAS. (**K**) Flowers of wild type, *an3-4*, *han-30* and *an3-4 han-30*. (**L-N**) Petal width (L), the number of cells in the transverse direction in petal epidermis (M) and the cell area of petal epidermis (N). Data are expressed as the mean±s.d. Scale bars: 1 mm in A-F,H,I,K; 100 μm in G; 1 cm in J.

Table 1. Frequencies of cotyledon phenotypes

Genotype	Cotyledon number (%)					n
	1	2	3	4	5	
Wild type	0	100	0	0	0	105
an3-4	0	99.32	0.68	0	0	294
#2047	0.14	87.01	11.49	1.08	0.29	1393

an3 and *#2047* mutants genetically interact during shoot development

The observed similarities in leaf phenotypes between *an3* and *#2047* suggest that *AN3* and the gene responsible for the *#2047* mutation play a similar role in leaf development. To explore this concept, we analysed the genetic interaction between *an3-4* and *#2047*. Surprisingly, *an3-4 #2047* double mutants exhibited more severe defects in shoot development than expected, based on the parental phenotypes (Fig. 2F). Many clusters of protrusions were observed in the region where cotyledons were normally formed. Some of these malformed protrusions were rod-like with trichomes (Fig. 2G), implying that these abnormal structures have leaf identities.

Nearly 25% of the progeny from plants that were heterozygous for *an3-4* and homozygous for the *#2047* mutation had abnormal shoot structures (49 of 200). This segregation ratio suggests that seedlings with abnormal shoots were doubly homozygous for *an3-4* and *#2047* mutations. The same shoot phenotype was confirmed in a combination of *an3-2* and *#2047* (Fig. 2H). Thus, the *an3* mutations caused a severe shoot defect when combined with the *#2047* mutation.

#2047 had a mutation in a GATA-type transcriptional factor gene, *HANABA TARANU* (*HAN*)

We performed map-based cloning and found that the mutation was located in the region between the PERL-0624941 and PERL-0625577 polymorphic markers on chromosome 3, which contains ~30 genes. Among them, we found a C-to-T substitution at nucleotide 211 from the initiator codon of *HAN*/*MONOPOLE* (*MNP*)/*GATA18*. *HAN* encodes a GATA-type transcriptional factor (Zhao et al., 2004; Nawy et al., 2010), and there are 29 loci for putative GATA factors in the *Arabidopsis* genome (Reyes et al., 2004). *HAN* has two closely related members, At2g18380/*GATA20* and At4g36620/*GATA19*. The mutation in *#2047* causes an amino acid substitution from Leu to Phe in a region specifically conserved among the three GATA transcription factor members (Zhao et al., 2004; supplementary material Fig. S1). Several *HAN* alleles have been characterised, but none had a mutation in this conserved region. To confirm that *HAN* is the mutated gene in *#2047*, we produced an *an3-4 han-1* double mutant and confirmed that it exhibited the same severe shoot defect to that in *an3-4 #2047* (Fig. 2I). Thus, we gave the name *han-30* to *#2047*.

Reproductive phenotypes of *an3 han-30*

The *an3 han* double mutant seedlings were not viable when sown on rock wool, but could be rescued when they are grown in vitro and then transferred to rock wool. Using this method, *an3 han-30* developed many leaves and produced flowers (Fig. 1D). The pollen produced by *an3 han-30* flowers was fertile (data not shown) and the flowers of *an3 han-30* did not set seeds (Fig. 2J,K). Petal and stamen numbers decreased in *han-30*, as reported in other *han* mutants (Table 2; Zhao et al., 2004). Organ number did not differ between *an3* and wild type (Table 2). The misregulation of sepal and petal numbers in *han-30* was influenced by the *an3* mutation; a significant increase in sepal number and a decrease in petal number were observed in the double mutant (Table 2). By contrast, the lower number of stamens in *han-30* was partially restored in *an3 han-30* (Table 2). The *an3* mutation did affect regulation of floral organ number in the *han-30* mutant, but the effect seemed to be different in each whorl.

We also examined the interaction between *an3* and *han-30* in terms of post-embryonic lateral organ development. An appropriate comparison of leaves in different mutants was difficult because *an3 han-30* had many more leaves than wild-type plants at the same developmental stage, probably owing to the occurrence of multiple shoots, and the size and number of cells in a leaf progressively changes according to node position (Usami et al., 2009). We instead examined petals, which are modified leaf organs. The widths of *an3-4*, *han-30* and *an3-4 han-30* petals were reduced to 71.6%, 85.2% and 52.0% compared with wild-type petals, respectively (Fig. 2L). Correspondingly, the number of adaxial epidermal cells along the transverse axis of *an3-4*, *han-30* and *an3-4 han-30* petals was reduced to 69.0%, 81.0% and 43.9% compared with wild-type petals, respectively (Fig. 2M). The petal cell number in *an3-4 han-30* was smaller than expected if we assume additive effects of the two mutations. The 43.9% reduction in cell number was less than the expected value of 55.9% (0.69×0.81). These results indicate that a synergistic interaction between *AN3* and *HAN* regulates cell proliferation in petals. Compensation occurred in the petals of all mutants examined, as seen in the leaves (Fig. 2M,N).

The *an3 han* seedling generates ectopic roots in the apical region

Next, we characterised developmental defects in late embryogenesis and post-germinative development in *an3 han-30*. The *an3-4 han-30* seeds were irregularly cone-shaped (Fig. 3A,B), which was due to a defect in cotyledon development and subsequent failure of cotyledon bending (Fig. 3C,D). *an3-4* seeds were small and had pale orange seed coats (supplementary material Fig. S2A,C), whereas *han-30* seeds were not significantly different from wild-type seeds (supplementary material Fig. S2B,D).

Surprisingly, some of the double mutant seedlings that germinated in vitro developed root-like protrusions in the apical region, in addition to the malformed leaf-like protrusions (Fig. 3F-

Table 2. Floral organ numbers

Genotype	Sepals		Petals		Stamens		Carpels		n
	Range	Mean±s.d.	Range	Mean±s.d.	Range	Mean±s.d.	Range	Mean±s.d.	
Wild type	4-5	4.02±0.14	4	4.00	5-6	5.84±0.37	2	2.00	50
an3-4	4	4.00	4	4.00	6	6.00	2	2.00	50
an3-2	4-5	4.02±0.14	4	4.00	5-6	5.94±0.24	2	2.00	50
han-30	3-5	4.18±0.66	2-5	3.28±0.73	3-6	4.68±0.77	2	2.00	50
an3-4 han-30	3-5	4.72±0.50	2-4	2.40±0.60	4-6	5.34±0.62	2-3	2.02±0.14	50
an3-2 han-30	3-5	4.64±0.56	2-4	2.62±0.67	4-6	5.28±0.73	2	2.00	50

The 10-23th flowers (n=50) on the primary meristem were scored. Fused organs were counted separately.

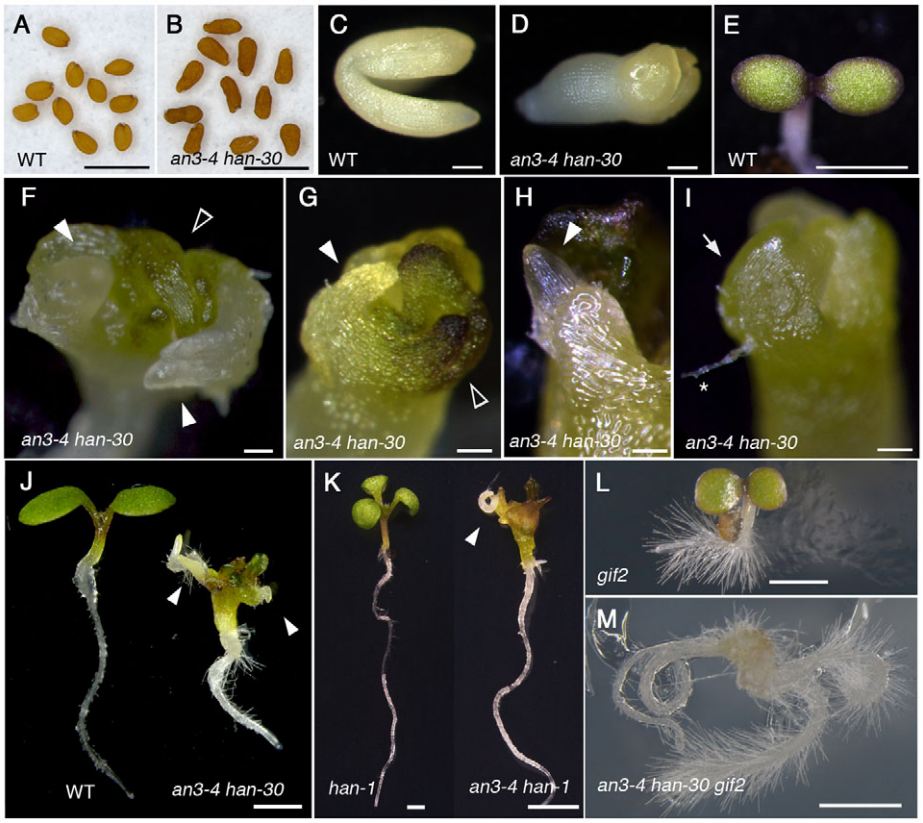

Fig. 3. *an3 han-30* double mutants produce ectopic roots in the apical region of seedlings. (**A-D**) Seeds of wild type (A) and *an3-4 han-30* (B). (C,D) Mature embryos of wild type (C) and *an3-4 han-30* (D). The seed coat was removed surgically. (**E-I**) The apical region of 4 DAS seedlings of wild type (E) and *an3-4 han-30* (F-I). Ectopic root-like structures (white arrowheads in F-H) often formed together with leaf-like structures (black arrowheads in F and G). Intermediate leaf and root structures (an arrow in I) were also observed in *an3-4 han-30*. Asterisk in I indicates a root hair. (**J**) The 5 DAS wild-type and *an3-4 han-30* seedlings. (**K**) The 12 DAS *han-1* and *an3-4 han-1* seedlings. Arrowheads in J and K indicate root-like structures. (**L**) The 4 DAS *gif2* seedling. (**M**) The 8 DAS putative *an3-4 han-30 gif2* seedling. Scale bars: 1 mm in A,B,E,J-M; 100 μm in C,D,F-I.

H) that were never observed in wild type, *an3-4* or *han-30* (Fig. 3E; supplementary material Fig. S2E,F). These root-like protrusions were white and had root hairs. Starch granules in a group of apical cells from these root-like protrusions stained similarly to primary roots (Fig. 4A-C; supplementary material Fig. S2G,H). Some leaf- and root-like protrusions were juxtaposed in the apical region (Fig. 3G). Moreover, intermediate structures between roots and leaves, which had root hairs but were green in colour, were occasionally observed (Fig. 3I). The penetrance rate of an abnormal root-like phenotype (including the intermediate phenotype) was ~50% (Table 3). After a prolonged in vitro culture (5 DAG), these root-like structures elongated as roots (Fig. 3J). This ectopic root phenotype was also observed in *an3-4 han-1* (Fig. 3K).

As *GIF* family members have redundant functions in leaf development (Lee et al., 2009), we examined the effect of the *gif2* mutation on the *an3 han* ectopic root phenotype. *gif2* never produced ectopic roots on the aerial parts (Fig. 3L). Strikingly, a subset of seedlings of the F2 progenies between *an3 han* and *gif2* showed even stronger transformation of cotyledons into roots (Fig. 3M) compared with that in *an3 han* seedlings (Fig. 3J,K). We carried out genotyping of 12 individuals from each of these abnormal seedlings with a moderate (like *an3-4 han-30* shown in Fig. 3J) or strong (Fig. 3M) phenotype. All seedlings were homozygous for *han-30* (supplementary material Table S1). Because *an3-4* is a deletion allele and its chromosome breakpoint is unknown (Horiguchi et al., 2005), *an3-4*/*AN3* and *AN3*/*AN3* genotypes are indistinguishable. Nevertheless, *gif2 an3 han* triple homozygous mutants were found only in seedlings with the strong phenotype (supplementary material Table S1), suggesting that *gif2* enhanced the *an3 han* ectopic root phenotype. We also investigated whether *GATA19* has a redundant role with *HAN*, and found that the *gata19* mutation did not significantly affect the *an3 han* phenotype (data not shown).

To determine whether intermediate and leaf-like protrusions also had some root-like features, we used the *pWOX5*::*GFP* reporter as a quiescent centre (QC) marker (Blilou et al., 2005). A GFP signal was observed only in the QC of primary roots of wild type, *an3-4* and *han-30* (Fig. 4D; supplementary material Fig. S2I,J). In *an3-4 han-30*, a GFP signal was observed at both the tip of the primary roots and the tip of root-like protrusions (Fig. 4E,F). In addition, a GFP signal was detectable as a spot in the intermediate type protrusions (Fig. 4G). We found that eight out of 30 *an3-4 han-30* seedlings had leaf-like protrusions with GFP signals. Leaf-like protrusions that had no GFP signal were also identified (six out of 30) (Fig. 4H). These results suggest that the root-like protrusions of the double mutants have root identity, and a subset of leaf-like protrusions might have a mixed root/leaf identity.

Development of *an3 han-30* embryos

To identify the primary defect of the *an3-4 han-30* double mutant, we analysed embryo development in *AN3*/*an3-4 han-30*/*han-30* plants and compared them with wild type, *an3-4* and *han-30* single-mutant embryos. Most embryos from *AN3*/*an3-4 han-30*/*han-30* plants did not exhibit aberrant cell division during early embryogenesis, but some embryos showed inappropriate cell division directions starting at the eight-cell stage (data not shown). Aberrant cell division was seen in only 9% of 16-cell stage embryos from *AN3*/*an3-4 han-30*/*han-30* plants (Table 4), similar to the frequency in the *han-30* single mutant (7.1%, Table 4), suggesting that there was no enhancement of aberrant cell division at the 16-cell stage by *an3-4* on *han-30*. A lens-shaped cell that is the progenitor of QC divided normally in all genotypes

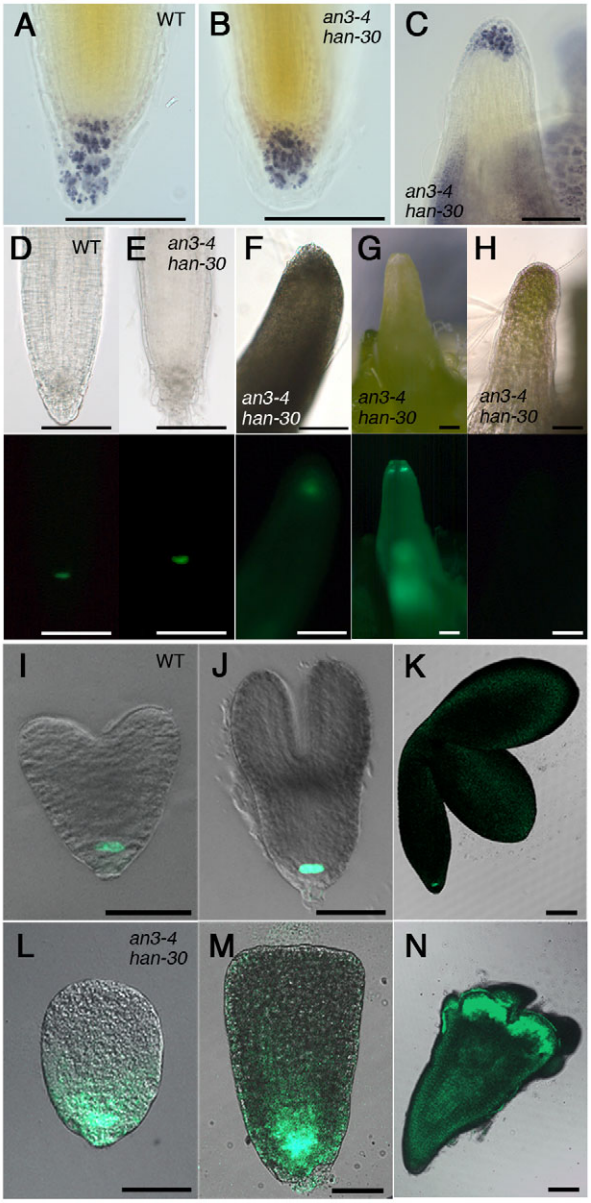

Fig. 4. Root-specific features observed in ectopic root-like structures in *an3-4 han-30* early seedlings and embryos. (**A-C**) Wild-type (A) and *an3-4 han-30* (B) root tips and an ectopic root-like structure (C) stained with Lugol's solution. (**D**,**E**) *pWOX5::GFP* expression in root tips of wild type (D) and *an3-4 han-30* (E). (**F-H**) *pWOX5::GFP* expression in an *an3-4 han-30* root-like structure (F) and an intermediate structure (G). No signal was detected in the leaf-like structures of *an3-4 han-30* (H). (**I-N**) *pWOX5::GFP* expression in wild type (I-K) and *an3-4 han-30* (L-N) during embryogenesis. Overlaid green fluorescent protein (green signal) and light microscopy images are shown. Heart-stage (I,L), torpedo-stage (J,M) and mature (K,N) embryos are shown. Scale bars: 50 μm in I,J,L,M; 100 μm in A-H,K,N.

(Fig. 5; supplementary material Fig. S2Q,R). A clear difference between mutants and wild-type embryos was observed at the heart stage, wherein *han-30* and some putative *an3-4 han-30* mutants showed retardation during development of organ primordia in the apical region (Fig. 5B; supplementary material Fig. S2R). Owing to the delayed primordia formation, some *han-30* and putative *an3-4 han-30* embryos were oval-shaped at the heart stage (Fig. 5B; supplementary material Fig. S2R). In *han-30*, cotyledons eventually developed (supplementary material Fig. S2D), whereas the *an3-4 han-30* embryos developed only small cotyledon-like structures at the end of embryo development (Fig. 3D).

Table 3. Frequencies of ectopic roots

Genotype	Seedlings with leaf-like structure only (%)	Seedlings with root-like and/or intermediate structures (%)	*n**
an3-4 han-30	51.11	48.89	90
an3-4 han-1	83.87	16.13	31

*Seedlings that show abnormal shoot structures were analysed.

Detection of shoot and root identities at the apical region of *an3 han* embryos

To determine when the ectopic root identity was established in the apical tissue of *an3-4 han-30*, we again applied the *pWOX5*::*GFP* reporter. Even in the heart stage, during which morphological defects were observed in *han-30* and *an3-4 han-30*, *pWOX5*::*GFP* was expressed only at the basal end of the embryo (Fig. 4I,L; supplementary material Fig. S2K,N). The area of *WOX5* expression was slightly expanded in *han-30* (supplementary material Fig. S2N; 60.0%, *n*=10), in oval-shaped embryos from *an3-4/an3-4 HAN/han-30* (Fig. 4L; 87.5%, *n*=16) and in some *an3-4* embryos (supplementary material Fig. S2K; 31.8%, *n*=22), but was always restricted to the basal part of the embryo. Similarly, no *pWOX5*::*GFP* expression was observed in the apical region in the torpedo stage in any of the mutants examined (Fig. 4J,M; supplementary material Fig. S2L,O). In mature embryos, in which organ primordia containing root-like protrusions were morphologically evident, ectopic *pWOX5::GFP* expression was detected in the apical part of the *an3-4 han-30* embryo (Fig. 4N) but not in wild type, *an3-4* or *han-30* (Fig. 4K; supplementary material Fig. S2M,P) embryos. This result indicates that ectopic root identity in *an3-4 han-30* is obtained during embryogenesis, but ectopic induction of *pWOX5*::*GFP* is not a primary cause of ectopic root formation.

To clarify whether the *an3 han* double mutant embryo has shoot identity in the apical region, we examined the expression pattern of the class III *HD-ZIP* gene *PHB* (Fig. 6). *PHB* mRNA was expressed in provascular cells and adaxial sides of cotyledon primordia and prospective SAM in all samples examined, as reported previously (McConnell et al., 2001). No difference in expression pattern was observed among wild-type, *an3-4* and *han-30* embryos (Fig. 6A-C). *PHB* mRNA was also detected in the apical region of a *han-30* oval-shaped embryo (data not shown). This expression in the apical region was detected in all embryos from *AN3/an3-4 han-30/han-30* that we examined (Fig. 6D-F, *n*=33), indicating that *PHB* mRNA accumulated in the apical region of the *an3-4 han-30* double mutant. This result suggests that the *an3 han-30* embryos retain shoot and cotyledon identities in their apical tissues.

The auxin accumulation pattern is not disrupted in *an3 han-30*

There are several reasons why ectopic roots form in the double mutant embryo. One possible explanation is that the defect in auxin accumulation leads to a disturbance of axial patterning. We used the *DR5rev::GFP* reporter to monitor the auxin response maxima in the embryos. During the globular stage in all genotypes

Table 4. Frequencies of aberrant cell division at the 16-cell stage

Parental genotype	%	*n*
Wild type	2.38	42
an3-4/an3-4	3.03	33
han-30/han-30	7.14	42
AN3/an3-4 han-30/han-30	8.96	67

examined, the GFP signal was visualised in the basal region, and no ectopic signal was observed in the apical region (Fig. 7, Table 5), suggesting that the apical-basal patterning was initiated relatively normally in *an3-4 han-30* at the globular stage as long as auxin response pattern concerns. At the heart stage, a more broadly distributed GFP signal was seen in the basal region of the *han-30* and *an3-4 han-30* embryos than in the wild-type and *an3-4* embryos, but was never detected in the apical region of any oval-shaped embryos of *han-30* or the putative *an3-4 han-30* (Fig. 7, Table 5). As cotyledon primordia develop during the late heart stage, the GFP signal was detected at the tip of the cotyledon primordia in wild type, *an3-4* and *han-30* (Fig. 7A-C). At this stage, *an3-4 han-30* embryos had a broad GFP signal in the apical region (Fig. 7D).

Misexpression of *PLT1* and its effect in *an3-4 han-30*

To determine the earliest molecular phenotypes in *an3-4 han-30* embryos, we examined the expression pattern of *PLT1* by in situ hybridisation. At the globular stage, *PLT1* was expressed in the provascular cells and in the lens-shaped QC progenitor cells of all genotypes examined (Fig. 8A,D,G,J), as reported by Aida et al. (Aida et al., 2004). We did not observe any differences in *PLT1* expression in the *an3-4* embryos (Fig. 8D-F). However, in *han-30*, a slightly broader pattern of *PLT1* expression was observed compared with wild-type samples (Fig. 8A,G), but it normalised during the heart stage (Fig. 8H,I compared with 8B,C). In most of the globular-stage putative *an3-4 han-30* embryos, the *PLT1* expression domain extended into the upper tiers (66.7%, *n*=15), whereas *PLT1* was never expressed there throughout embryogenesis in wild-type samples (Fig. 8A,J). This ectopic *PLT1* expression continued during subsequent developmental stages (Fig. 8B,K), then was gradually restricted to each primordium in the apical region (Fig. 8L,N). *PLT1* was not expressed in developing cotyledons in wild type (Fig. 8M). In summary, ectopic *PLT1* expression occurred earlier than the changes in apical auxin response, the induction of *pWOX5*::*GFP* misexpression and the patterning defect during embryogenesis.

We generated an *an3-4 han-30 plt1* triple mutant to evaluate the effect of *PLT1* misexpression in *an3 han*. The *plt1* mutation suppressed the ectopic root phenotype seen in *an3 han* (Fig. 8O,P). This suppression occurred in eight of 15 *plt1* heterozygous seedlings and in all of 60 *plt1* homozygous seedlings. The multiple shoot formation is also mostly suppressed. The narrow-leaf phenotype and sterility of *an3 han-30* did not recover by the *plt1* mutation (data not shown).

AN3 expression pattern in the embryo and the absence of a direct physical interaction between AN3 and HAN

HAN expression is observed broadly in early embryos until the globular stage and is gradually restricted to provascular tissues during subsequent stages of embryogenesis (Zhao et al., 2004; Nawy et al., 2010). We observed *AN3* expression during embryogenesis using *pAN3::GUS* to understand how *HAN* and *AN3* act to regulate embryogenesis. *AN3* was expressed in the basal half of globular-stage embryos but was absent in epidermal cells (supplementary material Fig. S3A). *AN3* was broadly expressed during the heart stage but not in the tips of the cotyledon primordia or in epidermal cells (supplementary material Fig. S3B). At later stages, *AN3* expression was observed in the basal region of cotyledon primordia, SAM, RAM and some provascular cells (supplementary material Fig. S3C,D). These expression patterns overlapped with those of *HAN* (Zhao et al., 2004; Nawy et al., 2010).

We next examined whether HAN and AN3 interact with each other using yeast two-hybrid assays (supplementary material Fig. S4). Neither wild-type HAN nor a mutant version of HAN (han-30) interacted with AN3. We also tested the interaction between HAN and GRF5, but no interaction was found.

DISCUSSION

In this study, we found that *an3/gif1* and *han* have phenotypic similarities in several aspects of leaf and floral organ development. Mutations in either gene inhibited cell proliferation in leaves, induced compensation and produced spoon-shaped leaves and a variable number of floral organs. *han* seedlings often have an altered number of cotyledons. This phenotype is also observed in *grf1 grf2 grf3* triple mutants that are defective in the interacting partners of AN3/GIF1 (Kim et al., 2003). More importantly, *an3* and *han* mutations genetically interact with each other and cause ectopic root formation in the apical region of the embryo where cotyledons normally develop. This phenotype is further enhanced by the *gif2* mutation. *PLT1* is ectopically expressed in the apical region of the *an3 han* embryo, and *plt1* suppresses the ectopic root phenotype. This suggests that the *HAN* and *GIF* family, represented by *AN3,* are cooperatively involved in regulating *PLT1* expression, which is required for establishing leaf identity during embryogenesis.

Here, we discuss the causes of ectopic root formation in *an3 han*. First, during embryogenesis, a disturbance in the auxin response pattern could cause disruption of the apical-basal axis,

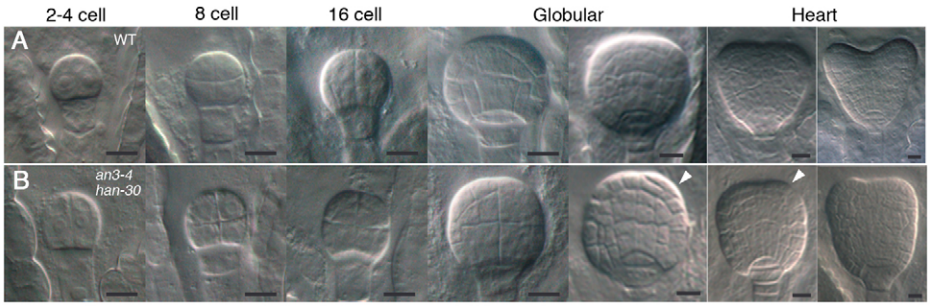

Fig. 5. Embryo development in *an3-4 han-30*. (**A**,**B**) The wild-type (A) and *an3-4 han-30* (B) embryos at the two- to four-cell to heart stages. Arrowheads indicate aberrant cell division. Scale bars: 10 μm.

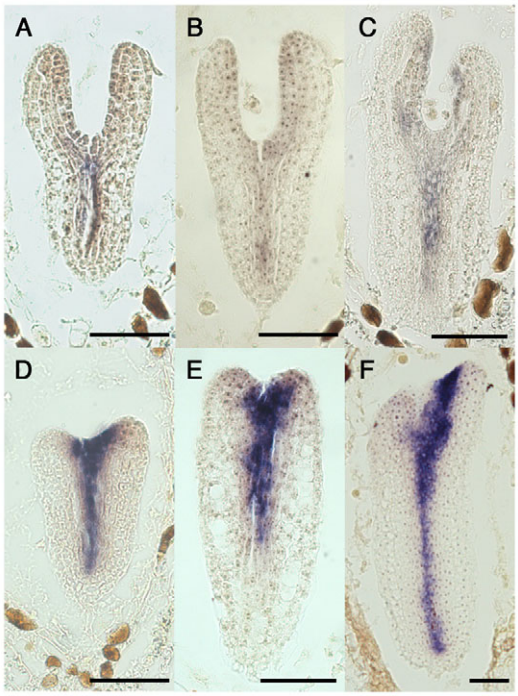

Fig. 6. Expression of *PHB* mRNA during embryogenesis. (**A-F**) *PHB* expression in wild type (A), *an3-4* (B), *han-30* (C) and *an3-4 han-30* (D-F) embryos in the late heart (D) and torpedo (A-C,E) stages and mature (F) embryos. Scale bars: 50 μm.

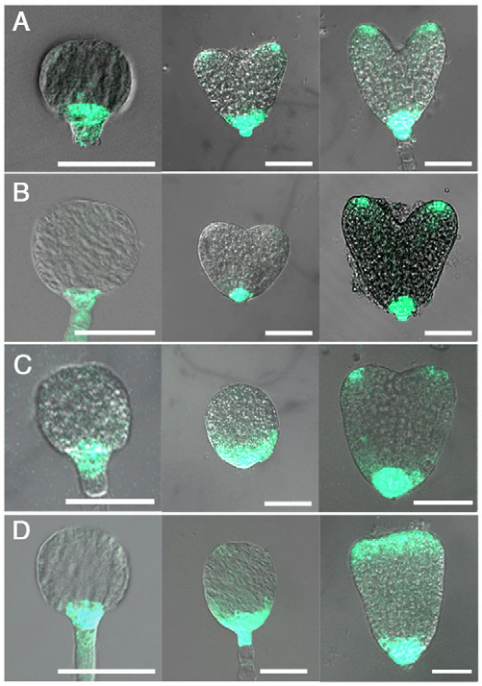

Fig. 7. Auxin response during embryogenesis. (**A-D**) *DR5rev::GFP* expression in wild-type (A), *an3-4* (B), *han-30* (C) and *an3-4 han-30* (D) embryos in the globular, heart and late heart stages (left to right in each panel). The heart-stage embryos in C,D are 'oval-shaped'. Overlays of GFP fluorescence with light microscopy images are shown. Scale bars: 50 μm.

leading to ectopic root formation. Polar auxin transport affects the expression of some genes, along with the apical-basal axis and other contributing developmental events (Blilou et al., 2005). However, our data do not support this possibility. Maximum DR5 activity was observed only in the basal region of the *an3-4 han-30* embryo in the globular stage, indicating that the relatively normal auxin response and apical-basal axis that requires an appropriate distribution of auxin are established once in *an3-4 han-30*. By contrast, Dhonukshe et al. (Dhonukshe et al., 2008) reported that increased auxin response in cotyledons stimulates the initiation of roots at cotyledon tips. In wild-type heart-stage embryos, polar auxin transport generates strong auxin maxima at the root pole and also creates weaker maxima at the cotyledon tips. Broad auxin accumulation in primordia of *an3-4 han-30* embryos was observed during the late heart stage. However, this accumulation occurred after patterning defects, such as retardation of organ primordia development and ectopic *PLT1* expression, which do not require auxin accumulation (Aida et al., 2004). Therefore, we consider this auxin response to be a secondary effect of altered embryonic development or the result of primordia formation. The final possible explanation for the formation of ectopic roots is the ectopic expression of a master regulator of root development. Ectopic expression of *PLT1* is sufficient to induce ectopic root formation (Aida et al., 2004; Galinha et al., 2007). Consistent with this finding, *PLT1* mRNA accumulated ectopically in the apical region of the *an3-4 han-30* embryo. *PLT*s are auxin-inducible genes (Aida et al., 2004), but *DR5rev::GFP* expression was normal when ectopic expression of *PLT1* was observed in early heart-stage embryos of *an3-4 han-30*. This result indicates that the ectopic expression of *PLT1* in *an3-4 han-30* was not induced by auxin. Additionally, the mutation in the *PLT1* gene fully suppressed the ectopic root phenotype seen in *an3 han*. Therefore, ectopic expression of *PLT1* is sufficient to account for ectopic root formation in *an3-4 han-30* embryos.

Table 5. *DR5rev::GFP* expression pattern in embryos

		Region of GFP signal		
Parental genotype	Stage	Basal	Basal and apical*	*n* (oval shaped)
Wild type	Globular	3	1	4
	Heart	10	0	10
an3-4/an3-4	Globular	8	1	9
	Heart	17	2	19
han-30/han-30	Globular	8	0	8
	Heart	35	0	35 (28)
an3-4/an3-4 HAN/han-30	Globular	21	1	22
	Heart	64	0	64 (21)

*Signals in the tip of the cotyledons were excluded.

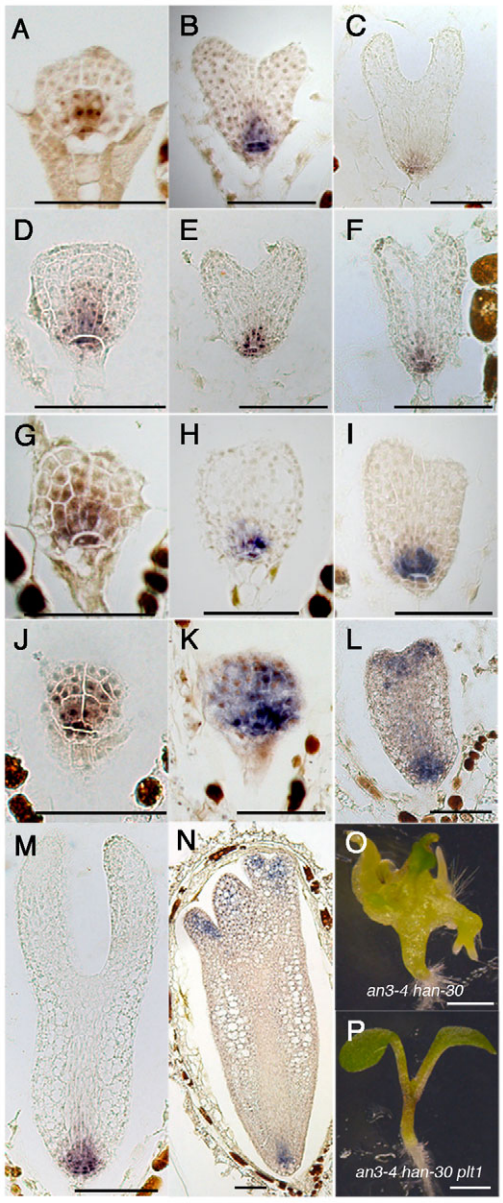

Fig. 8. Expression of *PLT1* mRNA during embryogenesis and the effects of *PLT1* misexpression in the *an3 han* mutant. (**A-N**) *PLT1* expression in wild-type (A-C,M), *an3-4* (D-F), *han-30* (G-I) and *an3-4 han-30* (J-L,N) embryos in the globular (A,D,G,J), heart (B,E,H,K), late heart (C,F,I,L) and torpedo (M) stages and mature (N) embryos. (**O**,**P**) The 4 DAS seedlings of *an3-4 han-30* (O) and *an3-4 han-30 plt1* (P). Scale bars: 50 μm in A-N; 1 mm in O,P.

The *han-30* mutant phenotype is similar to those of other *han* mutant alleles in terms of floral organ numbers (this study; Zhao et al., 2004), but there is a difference in the auxin response distribution pattern. The *DR5rev::GFP* signal shifted apically from the hypophysis during the globular stage in other *han* alleles, probably owing to misregulation of PIN1 and PIN7 (Nawy et al., 2010). However, in this study no significant changes were observed in either *han-30* or *an3-4 han-30* embryos. As *han-30* is probably a very weak allele that carries a missense mutation at a conserved region among *HAN*-like genes, it may not interfere with normal auxin distribution in developing embryos. *han-30* seems to have a similar or sufficient effect to the *han-1*-null allele in the *an3* background for ectopic root formation. We also found that the *gif2* mutation enhanced ectopic root formation in the *an3 han-30* background. Based on these findings, we propose that the *HAN* and *GIF* family, represented by *AN3*, coordinately repress *PLT1* expression in the apical region of embryos without auxin involvement, and repress ectopic root formation during embryogenesis. Genetic interaction analysis using a weak *han* allele and an *an3* mutant revealed that *HAN* could regulate *PLT1* expression, in addition to its previously reported role in regulating auxin distribution.

How *AN3* and *HAN* regulate *PLT1* expression is a key question to understand their roles in establishing cotyledon identity. *an3 han* double mutants induced severe defects in embryogenesis, which were not observed in either single mutant. It is interesting that the *AN3* and *HAN* expression domains partially overlapped during the globular stage (supplementary material Fig. S3A) (Zhao et al., 2004). However, HAN did not interact with AN3 or an AN3 interaction partner, GRF5, in yeast two-hybrid assays. These data suggest that *AN3*/*GRF5* and *HAN* function in parallel pathways and may have downstream targets that regulate *PLT1* expression through which cotyledon identity is stably established. *TPL* acts as a transcriptional co-repressor and negatively regulates *PLT* expression (Szemenyei et al., 2008; Smith and Long, 2010). As *AN3* is a putative transcriptional co-activator, *AN3* may positively regulate the expression of a negative regulator of *PLT1* expression. However, the role of HAN in transcriptional regulation is unknown. Some GATA members seem to be involved in both transcriptional activation and repression (Luo et al., 2010; Richter et al., 2010; Hudson et al., 2011). Further study is needed to understand the molecular mechanisms of AN3- and HAN-dependent repression of *PLT1* and whether *TPL* is involved in such mechanisms.

A second scenario is that *AN3* and/or *HAN* may positively regulate the genes required to stably establish cotyledon identity. We found that *PHB* was normally expressed at the adaxial side of abnormal organ primordia of the *an3-4 han-30* embryo. This suggests that *AN3* and *HAN* are not essential for deciding the fate of cotyledon development. As the *an3 gif2 han* triple mutant transformed the cotyledon into a root nearly completely, *AN3*, *GFI2* and *HAN* would play a role in stably establishing cotyledon identity in embryos. Their gradual loss of function might weaken cotyledon identity and then leak the root developmental program in the apical region of the mutant embryos. Thus, organ primordia in the apical region of the mutant embryos undergo both cotyledon and root developmental programs. This may explain why some protrusions of *an3 han* seedlings showed mixed root/cotyledon identity and delayed *WOX5* misexpression compared with *PLT1*. However, the mixed root/cotyledon identities seemed to be inconsistent with the finding concerning the mutual repression between root and shoot identity in apical meristems (Smith and Long, 2010). We believe that the ectopic root identity induced in *an3 han* is insufficient to suppress shoot identity completely or that *PHB* expression in cotyledons is not regulated by the same mechanism operating in the SAM. The molecular mechanisms that repress ectopic root formation via AN3 and HAN should be addressed in future studies.

AN3 is emerging as a key player in leaf development, as it promotes cell proliferation and adaxial identity, and coordinates cell proliferation and cell expansion (Kim and Kende, 2004; Horiguchi et al., 2005; Ferjani et al., 2007; Fujikura et al., 2007; Kawade et al., 2010; Horiguchi et al., 2011). In this study, we

demonstrate that both *AN3* and *HAN* are essential to repress root fate in cotyledon primordia during embryogenesis. Thus, *AN3* is an important factor that integrates multiple processes throughout leaf development.

Acknowledgements
We thank Dr E. Meyerowitz for providing the *han-1* seeds, Dr J. Friml for the *DR5rev::GFP* reporter line, Dr B. Scheres for the *pWOX5::GFP* reporter line, Dr A. Nakano for use of the confocal microscope and Dr S. Saiga for helpful advice.

Funding
This work was supported by grants-in-aid for Creative Scientific Research [18GS0313 to H.T.], Scientific Research on Priority Areas [19060002 to H.T.], Scientific Research A [17207005 to H.T. and G.H.], Exploratory Research [18657020 to G.H.], JSPS fellows from the Japan Society for the Promotion of Science [226978 to M.K.] and the Toray Science Foundation (H.T.).

Competing interests statement
The authors declare no competing financial interests.

Supplementary material
Supplementary material available online at
http://dev.biologists.org/lookup/suppl/doi:10.1242/dev.081547/-/DC1

References

Aida, M., Beis, D., Heidstra, R., Willemsen, V., Blilou, I., Galinha, C., Nussaume, L., Noh, Y. S., Amasino, R. and Scheres, B. (2004). The *PLETHORA* genes mediate patterning of the *Arabidopsis* root stem cell niche. *Cell* **119**, 109-120.

Alonso, J. M., Stepanova, A. N., Leisse, T. J., Kim, C. J., Chen, H., Shinn, P., Stevenson, D. K., Zimmerman, J., Barajas, P., Cheuk, R. et al. (2003). Genome-wide insertional mutagenesis of *Arabidopsis thaliana*. *Science* **301**, 653-657.

Beemster, G. T. S., Fiorani, F. and Inzé, D. (2003). Cell cycle: the key to plant growth control? *Trends Plant Sci.* **8**, 154-158.

Blilou, I., Xu, J., Wildwater, M., Willemsen, V., Paponov, I., Friml, J., Heidstra, R., Aida, M., Palme, K. and Scheres, B. (2005). The PIN auxin efflux facilitator network controls growth and patterning in *Arabidopsis* roots. *Nature* **433**, 39-44.

Byrne, M. E., Barley, R., Curtis, M., Arroyo, J. M., Dunham, M., Hudson, A. and Martienssen, R. A. (2000). *Asymmetric leaves1* mediates leaf patterning and stem cell function in *Arabidopsis*. *Nature* **408**, 967-971.

Chen, M., Liu, H., Kong, J., Yang, Y., Zhang, N., Li, R., Yue, J., Huang, J., Li, C., Cheung, A. Y. et al. (2011). *RopGEF7* regulates PLETHORA-dependent maintenance of the root stem cell niche in *Arabidopsis*. *Plant Cell* **23**, 2880-2894.

Dhonukshe, P., Tanaka, H., Goh, T., Ebine, K., Mähönen, A. P., Prasad, K., Blilou, I., Geldner, N., Xu, J., Uemura, T. et al. (2008). Generation of cell polarity in plants links endocytosis, auxin distribution and cell fate decisions. *Nature* **456**, 962-966.

Ferjani, A., Horiguchi, G., Yano, S. and Tsukaya, H. (2007). Analysis of leaf development in *fugu* mutants of Arabidopsis reveals three compensation modes that modulate cell expansion in determinate organs. *Plant Physiol.* **144**, 988-999.

Friml, J., Vieten, A., Sauer, M., Weijers, D., Schwarz, H., Hamann, T., Offringa, R. and Jürgens, G. (2003). Efflux-dependent auxin gradients establish the apical-basal axis of *Arabidopsis*. *Nature* **426**, 147-153.

Fujikura, U., Horiguchi, G. and Tsukaya, H. (2007). Dissection of enhanced cell expansion processes in leaves triggered by a defect in cell proliferation, with reference to roles of endoreduplication. *Plant Cell Physiol.* **48**, 278-286.

Fujikura, U., Horiguchi, G., Rosa Ponce, M., Luis Micol, J. and Tsukaya, H. (2009). Coordination of cell proliferation and cell expansion mediated by ribosome-related processes in the leaves of *Arabidopsis thaliana*. *Plant J.* **59**, 499-508.

Galinha, C., Hofhuis, H., Luijten, M., Willemsen, V., Blilou, I., Heidstra, R. and Scheres, B. (2007). PLETHORA proteins as dose-dependent master regulators of *Arabidopsis* root development. *Nature* **449**, 1053-1057.

Gallois, J. L., Nora, F. R., Mizukami, Y. and Sablowski, R. (2004). WUSCHEL induces shoot stem cell activity and developmental plasticity in the root meristem. *Genes Dev.* **18**, 375-380.

Gamborg, O. L., Miller, R. A. and Ojima, K. (1968). Nutrient requirements of suspension cultures of soybean root cells. *Exp. Cell Res.* **50**, 151-158.

Grigg, S. P., Galinha, C., Kornet, N., Canales, C., Scheres, B. and Tsiantis, M. (2009). Repression of apical homeobox genes is required for embryonic root development in *Arabidopsis*. *Curr. Biol.* **19**, 1485-1490.

Guo, M., Thomas, J., Collins, G. and Timmermans, M. C. P. (2008). Direct repression of *KNOX* loci by the ASYMMETRIC LEAVES1 complex of *Arabidopsis*. *Plant Cell* **20**, 48-58.

Horiguchi, G. and Tsukaya, H. (2011). Organ size regulation in plants: insights from compensation. *Front. Plant Sci.* **2**, 1-6.

Horiguchi, G., Kim, G.-T. and Tsukaya, H. (2005). The transcription factor AtGRF5 and the transcription coactivator AN3 regulate cell proliferation in leaf primordia of *Arabidopsis thaliana*. *Plant J.* **43**, 68-78.

Horiguchi, G., Fujikura, U., Ferjani, A., Ishikawa, N. and Tsukaya, H. (2006). Large-scale histological analysis of leaf mutants using two simple leaf observation methods: identification of novel genetic pathways governing the size and shape of leaves. *Plant J.* **48**, 638-644.

Horiguchi, G., Nakayama, H., Ishikawa, N., Kubo, M., Demura, T., Fukuda, H. and Tsukaya, H. (2011). *ANGUSTIFOLIA3* plays roles in adaxial/abaxial patterning and growth in leaf morphogenesis. *Plant Cell Physiol.* **52**, 112-124.

Hudson, D., Guevara, D., Yaish, M. W., Hannam, C., Long, N., Clarke, J. D., Bi, Y.-M. and Rothstein, S. J. (2011). *GNC* and *CGA1* modulate chlorophyll biosynthesis and glutamate synthase (*GLU1*/*Fd-GOGAT*) expression in *Arabidopsis*. *PLoS ONE* **6**, e26765.

Katoh, K., Misawa, K., Kuma, K. and Miyata, T. (2002). MAFFT: a novel method for rapid multiple sequence alignment based on fast Fourier transform. *Nucleic Acids Res.* **30**, 3059-3066.

Kawade, K., Horiguchi, G. and Tsukaya, H. (2010). Non-cell-autonomously coordinated organ size regulation in leaf development. *Development* **137**, 4221-4227.

Kim, J. H. and Kende, H. (2004). A transcriptional coactivator, AtGIF1, is involved in regulating leaf growth and morphology in *Arabidopsis*. *Proc. Natl. Acad. Sci. USA* **101**, 13374-13379.

Kim, J. H., Choi, D. and Kende, H. (2003). The AtGRF family of putative transcription factors is involved in leaf and cotyledon growth in *Arabidopsis*. *Plant J.* **36**, 94-104.

Kouchi, H. and Hata, S. (1993). Isolation and characterization of novel nodulin cDNAs representing genes expressed at early stages of soybean nodule development. *Mol. Gen. Genet.* **238**, 106-119.

Kumaran, M. K., Bowman, J. L. and Sundaresan, V. (2002). *YABBY* polarity genes mediate the repression of *KNOX* homeobox genes in Arabidopsis. *Plant Cell* **14**, 2761-2770.

Lee, B. H., Ko, J.-H., Lee, S., Lee, Y., Pak, J.-H. and Kim, J. H. (2009). The Arabidopsis *GRF-INTERACTING FACTOR* gene family performs an overlapping function in determining organ size as well as multiple developmental properties. *Plant Physiol.* **151**, 655-668.

Lin, W. C., Shuai, B. and Springer, P. S. (2003). The Arabidopsis *LATERAL ORGAN BOUNDARIES*-domain gene *ASYMMETRIC LEAVES2* functions in the repression of *KNOX* gene expression and in adaxial-abaxial patterning. *Plant Cell* **15**, 2241-2252.

Liu, D., Song, Y., Chen, Z. and Yu, D. (2009). Ectopic expression of miR396 suppresses *GRF* target gene expression and alters leaf growth in *Arabidopsis*. *Physiol. Plant.* **136**, 223-236.

Long, J. A., Woody, S., Poethig, S., Meyerowitz, E. M. and Barton, M. K. (2002). Transformation of shoots into roots in *Arabidopsis* embryos mutant at the *TOPLESS* locus. *Development* **129**, 2797-2806.

Long, J. A., Ohno, C., Smith, Z. R. and Meyerowitz, E. M. (2006). TOPLESS regulates apical embryonic fate in *Arabidopsis*. *Science* **312**, 1520-1523.

Luo, X.-M., Lin, W.-H., Zhu, S., Zhu, J.-Y., Sun, Y., Fan, X.-Y., Cheng, M., Hao, Y., Oh, E., Tian, M. et al. (2010). Integration of light- and brassinosteroid-signaling pathways by a GATA transcription factor in *Arabidopsis*. *Dev. Cell* **19**, 872-883.

McConnell, J. R., Emery, J., Eshed, Y., Bao, N., Bowman, J. and Barton, M. K. (2001). Role of *PHABULOSA* and *PHAVOLUTA* in determining radial patterning in shoots. *Nature* **411**, 709-713.

Murashige, T. and Skoog, F. (1962). A revised medium for rapid growth and bio assays with tobacco tissue cultures. *Physiol. Plant.* **15**, 473-497.

Nakayama, H., Yamaguchi, T. and Tsukaya, H. (2010). Expression patterns of AaDL, a CRABS CLAW ortholog in *Asparagus asparagoides* (Asparagaceae), demonstrate a stepwise evolution of CRC/DL subfamily of YABBY genes. *Am. J. Bot.* **97**, 591-600.

Nawy, T., Bayer, M., Mravec, J., Friml, J., Birnbaum, K. D. and Lukowitz, W. (2010). The GATA factor *HANABA TARANU* is required to position the proembryo boundary in the early *Arabidopsis* embryo. *Dev. Cell* **19**, 103-113.

Ori, N., Eshed, Y., Chuck, G., Bowman, J. L. and Hake, S. (2000). Mechanisms that control *knox* gene expression in the *Arabidopsis* shoot. *Development* **127**, 5523-5532.

Relichova, J. (1976). Some new mutants. *Arabidopsis Inf. Serv.* **13**, 25-28.

Reyes, J. C., Muro-Pastor, M. I. and Florencio, F. J. (2004). The GATA family of transcription factors in Arabidopsis and rice. *Plant Physiol.* **134**, 1718-1732.

Richter, R., Behringer, C., Müller, I. K. and Schwechheimer, C. (2010). The GATA-type transcription factors GNC and GNL/CGA1 repress gibberellin signaling downstream from DELLA proteins and PHYTOCHROME-INTERACTING FACTORS. *Genes Dev.* **24**, 2093-2104.

Rodriguez, R. E., Mecchia, M. A., Debernardi, J. M., Schommer, C., Weigel, D. and Palatnik, J. F. (2010). Control of cell proliferation in *Arabidopsis thaliana* by microRNA miR396. *Development* **137**, 103-112.

Sarojam, R., Sappl, P. G., Goldshmidt, A., Efroni, I., Floyd, S. K., Eshed, Y. and Bowman, J. L. (2010). Differentiating Arabidopsis shoots from leaves by combined YABBY activities. *Plant Cell* **22**, 2113-2130.

Semiarti, E., Ueno, Y., Tsukaya, H., Iwakawa, H., Machida, C. and Machida, Y. (2001). The *ASYMMETRIC LEAVES2* gene of *Arabidopsis thaliana* regulates formation of a symmetric lamina, establishment of venation and repression of meristem-related homeobox genes in leaves. *Development* **128**, 1771-1783.

Smith, Z. R. and Long, J. A. (2010). Control of *Arabidopsis* apical-basal embryo polarity by antagonistic transcription factors. *Nature* **464**, 423-426.

Szemenyei, H., Hannon, M. and Long, J. A. (2008). TOPLESS mediates auxin-dependent transcriptional repression during *Arabidopsis* embryogenesis. *Science* **319**, 1384-1386.

Tsuge, T., Tsukaya, H. and Uchimiya, H. (1996). Two independent and polarized processes of cell elongation regulate leaf blade expansion in *Arabidopsis thaliana* (L.) Heynh. *Development* **122**, 1589-1600.

Tsukaya, H. (2002). Interpretation of mutants in leaf morphology: genetic evidence for a compensatory system in leaf morphogenesis that provides a new link between cell and organismal theories. *Int. Rev. Cytol.* **217**, 1-39.

Tsukaya, H. (2008). Controlling size in multicellular organs: focus on the leaf. *PLoS Biol.* **6**, 1373-1376.

Usami, T., Horiguchi, G., Yano, S. and Tsukaya, H. (2009). The *more and smaller cells* mutants of *Arabidopsis thaliana* identify novel roles for *SQUAMOSA PROMOTER BINDING PROTEIN-LIKE* genes in the control of heteroblasty. *Development* **136**, 955-964.

Wang, L., Gu, X., Xu, D., Wang, W., Wang, H., Zeng, M., Chang, Z., Huang, H. and Cui, X. (2011). miR396-targeted AtGRF transcription factors are required for coordination of cell division and differentiation during leaf development in *Arabidopsis*. *J. Exp. Bot.* **62**, 761-773.

Zhao, Y., Medrano, L., Ohashi, K., Fletcher, J. C., Yu, H., Sakai, H. and Meyerowitz, E. M. (2004). HANABA TARANU is a GATA transcription factor that regulates shoot apical meristem and flower development in *Arabidopsis*. *Plant Cell* **16**, 2586-2600.

Table S1. Genotyping of segeregants in F2 progenies of *an3-4 han-30* × *gif2*

Genotype	Moderate phenotype*	Strong phenotype‡
han/*han gif2*/*GIF2 AN3* (*an3*/*AN3* or *AN3*/*AN3*)	6	5
han/*han gif2*/*gif2 AN3* (*an3*/*AN3* or *AN3*/*AN3*)	5	3
han/*han gif2*/*GIF2 an3*/*an3*	1	2
han/*han gif2*/*gif2 an3*/*an3*	0	2

*Number of segregants with abnormal shoots with green tissues.

‡Number of segregants with strong transformation of cotyledons into roots.